JMEPEG (2015) 24:1026–1030
DOI: 10.1007/s11665-014-1354-4

1059-9495/$19.00

Microstructural and Hardness Changes during Isothermal Annealing of Nanostructured Al-11.6Fe-1.3V-2.3Si Alloy

H. Ashrafi, R. Emadi, and M.H. Enayati

(Submitted August 8, 2014; in revised form November 13, 2014; published online December 10, 2014)

Microstructural evolution and hardness change during isothermal annealing (300-550 °C, 30 min) of nanostructured Al-11.6Fe-1.3V-2.3Si alloy, prepared by mechanical alloying (MA) of elemental powders, were investigated using x-ray diffraction, transmission electron microscopy, and Vickers microhardness test. The results showed that the microstructure of the alloy after 60 h of MA consisted of a nanostructured Al-based solid solution with embedded Si. Annealing of the as-milled powders led to grain growth, internal strain release, and precipitation of the $Al_{12}(Fe,V)_3Si$ compound above 400 °C. The grain growth of Al enhanced above the onset temperature for the precipitation of $Al_{12}(Fe,V)_3Si$ phase. The grain size of Al after 30 min of annealing at 550 °C reached ~50 nm. Solute drag was responsible for retarding the grain growth below 400 °C, and above that temperature the grain growth was mainly limited by second-phase drag. The hardness (219 HV) of as-milled Al-11.6Fe-1.3V-2.3Si alloy decreased after annealing at 300 °C, but above that temperature the hardness increased with increasing the annealing temperature and reached ~250 HV after annealing at 550 °C for 30 min.

Keywords Al-Fe-V-Si alloy, grain growth, hardness, isothermal annealing, nanostructured material, precipitation

1. Introduction

Al-Fe-V-Si alloys are of the best high temperature aluminum alloys because of their good room and high temperature strength, ductility, fracture toughness, and excellent thermal stability. The microstructure of these alloys, which are usually processed via rapid solidification methods, consists of nearly spherical dispersions of $Al_{12}(Fe,V)_3Si$ phase in a fine-grained Al matrix. This intermetallic phase is responsible for the good properties of the rapidly solidified Al-Fe-V-Si alloys (Ref 1, 2).

Nanostructured materials have been the subject of intensive study over the past years owing to their unique properties compared with coarse-grained materials (Ref 3). Mechanical alloying (MA) is a widely used method for synthesis of nanostructured materials (Ref 4). Because the product of MA is in the form of powder, subsequent consolidation is necessary to obtain a fully dense bulk sample. Conventional consolidation processes are usually performed at high temperatures or include a heating step (Ref 4). Therefore, grain growth and phase transformation can occur during the consolidation process and affect the properties of final bulk material. Because of these problems, many studies have been devoted to the thermal stability of nanostructured materials (Ref 5-9). These studies demonstrated that nanostructured materials have limited grain growth because of a number of factors that affect the grain boundary mobility. These factors include: solute drag, second-phase drag, and grain boundary segregation (Ref 6). Beside grain growth, other phenomena like internal strain release and phase transformation (second-phase precipitation) can also occur upon the heating of nanostructured materials which can have an effect on their properties.

In our previous works (Ref 10, 11), we produced the bulk nanocrystalline Al-Fe-V-Si alloys by MA and subsequent hot pressing of elemental powders and studied their room and high temperature mechanical properties and their thermal stability. Because exposure to high temperatures is unavoidable in the production of bulk nanocrystalline samples from the mechanically alloyed Al-Fe-V-Si powders, it is necessary to know the structural evolutions which take place upon heating of the milled powder and their effects on the mechanical properties. Based on the above, the aim of the present study was to investigate the microstructural evolutions and hardness change during the isothermal annealing of the mechanically alloyed Al-11.6Fe-1.3V-2.3Si powder at different temperatures.

2. Experimental Procedures

The powders of Al (99.5% purity), Fe (99.8% purity), V (99.5% purity), and Si (99.8% purity) with nominal composition of Al-11.6Fe-1.3V-2.3Si (wt.%) were used as starting materials. The MA was performed in a high energy planetary ball mill at room temperature under argon atmosphere for 60 h. In order to prevent severe sticking of aluminum powders to the balls and vial, 1.5 wt.% of stearic acid was used as the process control agent. After the MA, the powders were heat treated to investigate the structural changes during the subsequent

H.Ashrafi, R.Emadi, and **M.H.Enayati,** Department of Materials Engineering, Isfahan University of Technology, Isfahan 84156-83111, Iran. Contact e-mail: h.ashrafi@ma.iut.ac.ir.

heating. For this purpose, a small amount of powders were placed in a sealed capsule and then annealed at temperatures between 300 and 550 °C for 30 min in a conventional furnace. After the heat treatment, the capsule was cooled in the air. Structural changes after annealing were determined by x-ray diffraction (XRD) in a Philips X' PERT MPD diffractometer using filtered Cu Kα radiation (λ = 0.15406 nm). The XRD patterns were recorded in the 2θ range of 10-90° (step size 0.05°, time per step 1 s). The grain size and internal strain of powders were evaluated from the broadening of XRD peaks using the Williamson-Hall method (Ref 12):

$$\beta \cos \theta = \frac{0.9\lambda}{d} + 2\varepsilon \sin \theta, \qquad \text{(Eq 1)}$$

where β is peak full width at half maximum intensity, λ is the wavelength of the x-ray (0.15406 nm), θ is the Bragg angle, d is the average grain size, and ε is the average internal strain.

Microstructure of the heat-treated powders was examined by transmission electron microscopy (TEM). The TEM sample was prepared by suspending the powder in ethanol using ultrasonic vibration. A drop of the suspension was then placed on a carbon-coated copper grid and dried. The sample was investigated using a 120 kV Philips CM120 transmission electron microscope. Microhardness tests were conducted on the cross section of the powder particles using a Vickers indenter at a load of 25 g. The microhardness samples were prepared by mounting a small amount of powder in a carbon-based resin followed by grinding and polishing.

3. Results and Discussion

3.1 XRD Results

Figure 1 shows the XRD patterns of as-milled Al-11.6Fe-1.3V-2.3Si powder mixture and also after annealing at 300, 400, 500, and 550 °C for 30 min. It was indicated in our previous study that after 60 h of MA, the mixed powder consisted of nanostructured Al solid solution with a grain size of 19 nm and an internal strain level of ~0.55% in which Si phase was embedded (Ref 13). Reduction of grain size during the MA increases grain boundary area and reduces diffusion distances that can facilitate formation of intermetallics on a subsequent heat treatment.

According to Fig. 1, after 30 min of annealing at 300 °C, no new phase was formed from the as-milled powder and the structure consisted of the nanostructured Al solid solution. Si peaks was also observed in the XRD pattern. By 30 min of annealing at 400 °C, $Al_{12}(Fe,V)_3Si$ peaks were observed in the XRD pattern and the Si peaks were disappeared. The disappearance of Si peaks is due to the transfer of this element to the $Al_{12}(Fe,V)_3Si$ intermetallic compound by the precipitation reaction. By increasing the annealing temperature to 500 °C, the intensity of $Al_{12}(Fe,V)_3Si$ peaks increased. This is because the precipitation enhanced at higher temperatures. By increasing the annealing temperature to 550 °C, the intensity of $Al_{12}(Fe,V)_3Si$ XRD peaks only increased slightly. It is worth mentioning that undesirable phases were not observed after annealing at any of the mentioned temperatures.

The lattice parameter of Al was calculated based on the Nelson-Riley method [14] by plotting the value of lattice parameter computed for each peak versus the Nelson-Riley function and extrapolating the line passed from them to the point where the Nelson-Riley function becomes zero. Figure 2 shows the lattice parameter of Al as a function of the temperature for 30 min anneal. The lattice parameter of Al in the as-milled condition was 0.4041 nm, which is substantially lower than that of pure Al. This is because of the dissolution of Fe, V, and Si atoms in the Al lattice and formation of an Al(Fe,V,Si) solid solution (Ref 13).

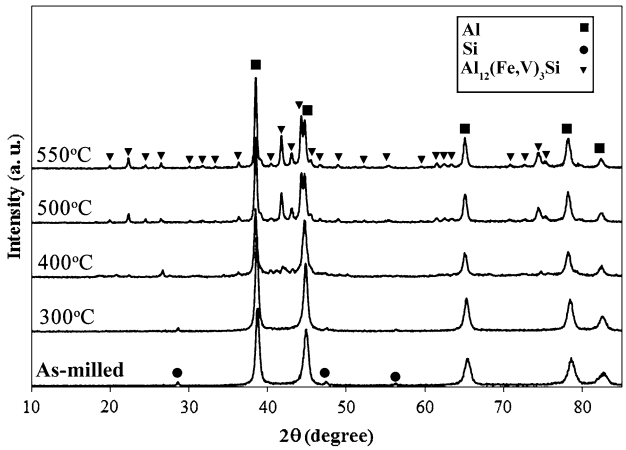

Fig. 1 XRD patterns of 60 h-milled Al-11.6Fe-1.3V-2.3Si alloy after 30 min of annealing at various temperatures

According to Fig. 2, the lattice parameter of Al remained unchanged after annealing at 300 °C. This is consistent with the XRD result in Fig. 1 which indicated that the Al-based solid solution was still stable after 30 min of annealing at 300 °C.

Figure 2 shows that the Al lattice parameter increased after annealing at 400 °C. This is due to the rejection of smaller Fe, V, and Si atoms from the Al lattice and formation of the $Al_{12}(Fe,V)_3Si$ intermetallic compound. However, as Fig. 2 shows, the lattice parameter of sample annealed at 400 °C was lower than the lattice parameter of pure Al, indicating that some of the Fe, V, and Si atoms still remained in solution with Al. Annealing at 500 °C caused further increase in the lattice parameter. As can be seen, the Al lattice parameter has a sharp increase at this temperature but still is slightly lower than the lattice parameter of pure Al. This shows that most of the Fe, V, and Si atoms were rejected from the solid solution and formed $Al_{12}(Fe,V)_3Si$ phase. After 30 min of annealing at 550 °C, the lattice parameter of Al reached to the lattice parameter of pure Al. This indicates that nearly all the solute elements were rejected from the Al matrix and formed the $Al_{12}(Fe,V)_3Si$ precipitates. Considering the XRD results and lattice parameter changes, and by assuming that the precipitation was completed at 550 °C, the volume fraction of $Al_{12}(Fe,V)_3Si$ phase formed in each temperature was estimated and included in Fig. 2.

It has been shown by previous researches that nano grains, high level of internal strain, and supersaturation are all metastable (Ref 5), therefore precipitation would expected upon heating of the MA-processed Al-11.6Fe-1.3V-2.3Si alloy. The onset temperature of precipitation depends strongly on the diffusion coefficient of the alloying elements involved in the precipitation. The lattice diffusion length of an element is obtained by the Einstein equation (Ref 15):

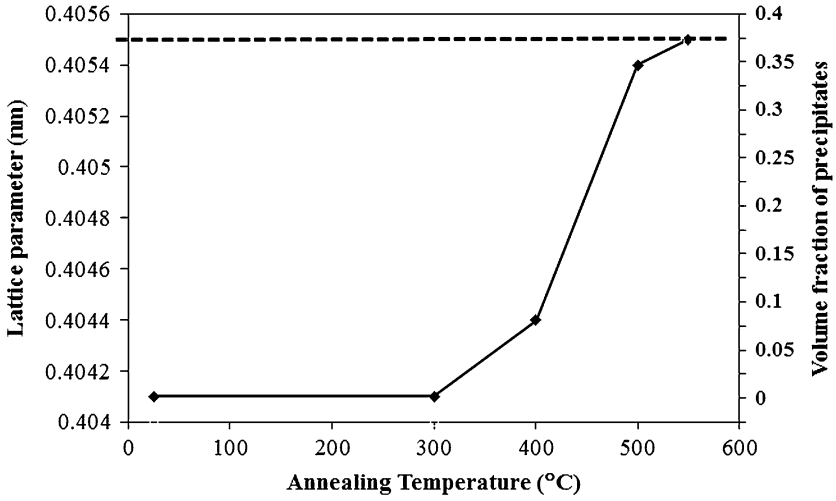

Fig. 2 The lattice parameter of Al in Al-11.6Fe-1.3V-2.3Si powder after 60 h of MA and annealing at different temperatures for 30 min. The dashed line indicates the lattice parameter of pure Al. The right axis illustrates the volume fraction of $Al_{12}(Fe,V)_3Si$ precipitates

Table 1 Diffusion data for Fe in solid Al [21]

D at 300 °C, m^2/s	$\sqrt{R^2}$ at 300 °C, nm	D at 400 °C, m^2/s	$\sqrt{R^2}$ at 400°C, nm
1.12×10^{-20}	4.5	8.88×10^{-18}	126

$$\sqrt{R^2} = \sqrt{6Dt}, \quad \text{(Eq 2)}$$

where $\sqrt{R^2}$ is the lattice diffusion length, D is the diffusion coefficient, and t is the time. Table 1 shows the diffusion data and lattice diffusion length for Fe at 300 and 400 °C in 30 min. According to Table 1, the lattice diffusion length for Fe at 300 and 400 °C in 30 min is 4.5 and 126 nm, respectively. This result suggests that the mobility of Fe, which is the main alloying element in the studied alloy, is not enough at 300 °C for precipitation to occur, but it is high enough at 400 °C. According to the XRD results, the onset temperature for precipitation was 400 °C, which is in agreement with the diffusion data.

3.2 Grain Growth

Figure 3 shows the changes in Al grain size and internal strain at different annealing temperatures. It is observed that the grain size of Al increased with increasing the annealing temperature. The grain size of Al changed little below 400 °C, but above it the grain growth became more significant. Internal strain decreased in a constant rate with raising the annealing temperature. This alloy appeared to have good thermal stability upon annealing so that the initial grain size of 19 nm for the as-milled sample increased to 49 nm after 30 min of annealing at 550 °C ($\sim 0.9T_m$).

The enhancement of grain growth above the onset temperature for the precipitation of $Al_{12}(Fe,V)_3Si$ compound is suggested that solute drag is responsible for retarding the grain growth below 400 °C and at temperatures above 400 °C, due to the precipitation of $Al_{12}(Fe,V)_3Si$ intermetallic phase, the grain growth is mainly limited by the second-phase drag. Segregation of solute atoms at grain boundaries reduces the grain boundary mobility and grain boundary energy, therefore hindering the grain growth. The drag force excreted by the solute atoms is proportional to the diffusion coefficient of the solute atoms and the difference between the solute concentration at the grain boundary and in the grain interior (Ref 5). According to Table 1, the lattice diffusion length for Fe, the main alloying element, at 300 °C in 30 min is only 4.5 nm. Therefore, because the grain growth of Al requires diffusion of the Fe, V, and Si atoms, the grain growth of Al will be limited at 300 °C. However, the lattice diffusion length for Fe at 400 °C in 30 min is 126 nm. Therefore, significant grain growth of Al at 400 °C becomes possible. According to the XRD results, the precipitation of $Al_{12}(Fe,V)_3Si$ occurred at 400 °C, therefore second-phase drag impedes the grain growth of Al at temperatures higher than 400 °C, and solid solution drag becomes less important. The effect of solid solution drag diminishes with increasing the temperature to 550 °C.

According to Fig. 3, the grain growth of Al is more significant between 400 and 500 °C where most of the precipitation of $Al_{12}(Fe,V)_3Si$ compound occurred (Fig. 2). Therefore, it can be concluded that the grain growth is accelerated by the precipitation of second phase. It has been shown that the decrease of solute drag during the precipitation can led to an acceleration of grain growth, especially in very fine-grained or nanocrystalline materials (Ref 16).

Figure 4 shows the TEM image of the sample annealed at 550 °C for 30 min, after which the precipitation was almost completed. At this temperature, only the second-phase drag can retard the grain growth of Al. According to the Zener equation, the maximum grain size obtained in the presence of second-phase particles can be obtained from the following equation (Ref 17):

$$d_m = \frac{4r}{3f}, \quad \text{(Eq 3)}$$

where d_m is the grain size after grain growth occurred completely, r is the mean radius of second-phase particles, and f is the volume fraction of pinning particles. The second-phase particles in the TEM image have a diameter between 10 and

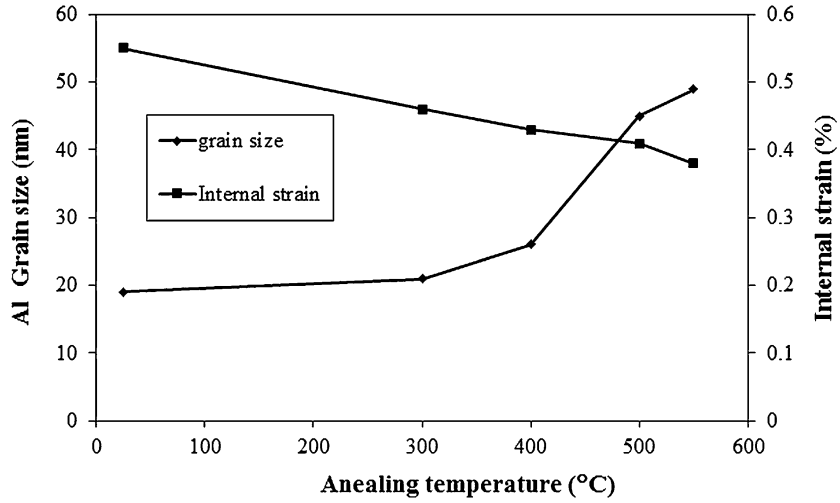

Fig. 3 Grain size of Al in the Al-11.6Fe-1.3V-2.3Si alloy after 60 h of MA and 30 min of annealing at various temperatures

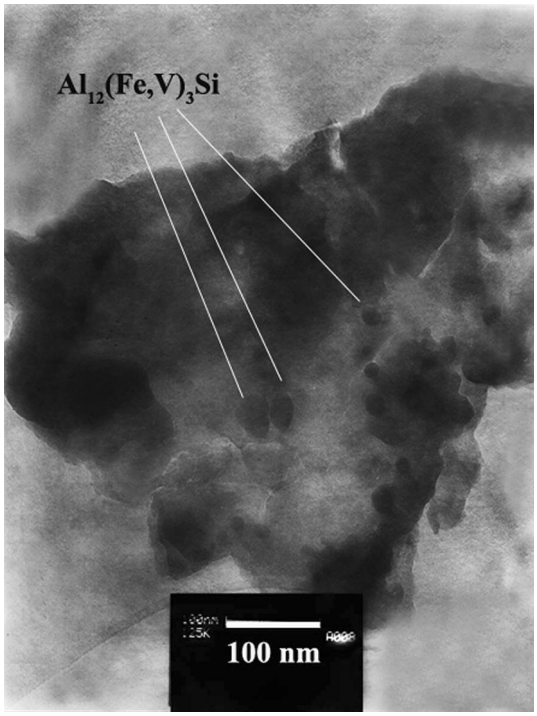

Fig. 4 TEM bright field image of the Al-11.6Fe-1.3V-2.3Si alloy powder after 60 h of MA and annealing at 550°C for 30 min

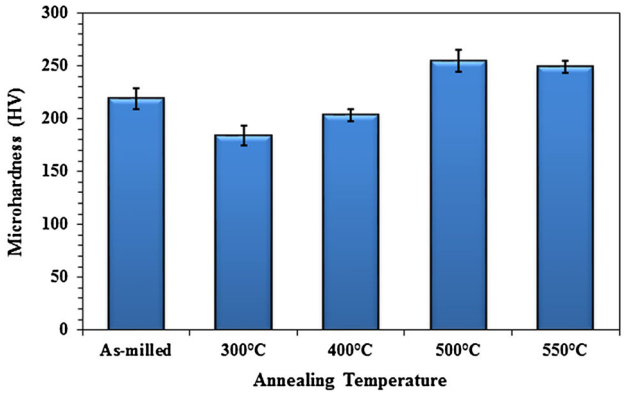

Fig. 5 Room temperature Vickers hardness of mechanically alloyed Al-11.6Fe-1.3V-2.3Si alloy powder after 30 min of annealing at various temperatures

40 nm and a mean diameter of ~25 nm. Taking $f = 0.37$ (nominal value) and $r = 12.5$, Eq 3 led to a mean grain size of ~45 nm, a value close to the grain size (49 nm) obtained from the Williamson-Hall method.

3.3 Hardness Changes

Figure 5 shows the Vickers hardness of the as-milled Al-11.6Fe-1.3V-2.3Si alloy powders after annealing at different temperatures for 30 min. The average hardness value of the alloy powder after 60 h of MA was 219 HV. This high hardness value in the as-milled condition is mainly resulted from three effects: solid solution hardening, very small grain size, and relatively high level of internal strain. Note that by 30 min of annealing at 300 °C, the hardness value decreased to 184 HV, but above 300 °C the hardness increased with increasing the temperature of 30 min anneal. The decrease in hardness at 300 °C is attributed to the grain growth and release of internal strain (Fig. 3). At 400 °C, the hardness increased compared with that after annealing at 300 °C, due to the precipitation of $Al_{12}(Fe,V)_3Si$ intermetallic phase (Fig. 1). In fact, at this temperature grain growth and release of internal strain still tend to reduce the hardness value, but the effect of $Al_{12}(Fe,V)_3Si$ precipitates in increasing the hardness predominates and the hardness value increases. Annealing at 500 °C led to further increase in hardness so that, after annealing at this temperature the hardness value reached to ~255HV, which is even higher than the hardness value in the as-milled condition. The further increase in hardness at 500 °C is caused by the formation of more precipitates of $Al_{12}(Fe,V)_3Si$ intermetallic compound (Fig. 2). As can be seen in Fig. 5, annealing at 550 °C had no significant effect on the hardness. The above results indicate that if high strength is desirable, consolidation must performed in the temperature range of 500-550 °C.

The hardness increase after the precipitation of $Al_{12}(Fe,V)_3Si$ intermetallic compound is resulted from two parameter: high volume fraction of precipitates and their very small size (Fig. 4). According to the second-phase hardening theories, the strength increase due to the presence of second-phase particles is directly proportional to their volume fraction and inversely proportional to their size (Ref 18). Here because of a high volume fraction (0.37) and very small size (d ~25 nm), the $Al_{12}(Fe,V)_3Si$ precipitates had a strong influence on hardness and could compensate the hardness reduction caused by the loss of solid solution hardening, grain growth, and release of internal strains at higher temperatures.

The results obtained here were not completely in line with the results of other works. Shaw et al. (Ref 19) reported that the hardness of MA-processed $Al_{93}Fe_3Ti_2Cr_2$ alloy decreased after annealing at temperatures up to 450 °C, where precipitation of intermetallics occurred above 300 °C. Nayak et al. (Ref 20) observed that the hardness value of 20 h mechanically alloyed Al-Fe alloys increased after annealing at temperatures up to 400 °C, but decreased after annealing at temperatures above 400 °C. They attributed the increase in hardness to the precipitation of intermetallic compounds and the hardness reduction to the coarsening of microstructure and annihilation of defects being created during MA.

4. Conclusions

In the present study, microstructural and hardness changes during the isothermal annealing of 60 h mechanically alloyed Al-11.6Fe-1.3V-2.3Si powder at temperatures between 300 and 550 °C were investigated. The following results were drawn:

- The microstructure of powder after MA consisted of a nanostructured Al-based solid solution in which Si phase was embedded.
- Annealing of the as-milled Al-11.6Fe-1.3V-2.3Si alloy led to three important phenomena: precipitation of the $Al_{12}(Fe,V)_3Si$ phase, grain growth, and internal strain release.
- No phase transformation occurred after annealing at 300 °C, but $Al_{12}(Fe,V)_3Si$ phase precipitated after annealing at 400 °C and its volume fraction increased with increasing the annealing temperature to 550 °C.
- The grain growth of Al enhanced above the onset temperature for the precipitation of $Al_{12}(Fe,V)_3Si$ compound. The grain size of Al after 30 min of annealing at 550 °C reached to ~50 nm. Solute drag is responsible for retarding the grain growth below 400 °C, and above that temperature the grain growth mainly limited by second-phase drag.
- The hardness of as-milled Al-11.6Fe-1.3V-2.3Si alloy (219 HV) decreased after annealing at 300 °C, but above that temperature the hardness increased by increasing the annealing temperature and reached to ~250 HV after annealing at 550 °C for 30 min.

References

1. R.H. Zhang, B.H. Zho, Y.A. Zhang, and B. Wu, Effect of Temperature on Microstructure and Mechanical Properties of Spray Forming Al-8.5 Fe-1.3V-1.7Si Alloys, *Adv. Mater. Res.*, 2011, **287-290**, p 43–48
2. W.A. Baeslack, K.V. Jata, and T.J. Lienert, Structure, Properties and Fracture of Friction Stir Welds in a High-Temperature Al-8.5Fe-1.3 V-1.7Si Alloy (AA-8009), *J. Mater. Sci.*, 2006, **41**, p 2939–2951
3. A.M. Soufiani, F. Karimzadeh, and M.H. Enayati, Formation Mechanism and Characterization of Nanostructured Ti6Al4V Alloy Prepared by Mechanical Alloying, *Mater. Des.*, 2012, **37**, p 152–160
4. M. Krasnowski, A. Antolak-Dudka, and T. Kulik, Bulk Amorphous $Al_{85}Fe_{15}$ Alloy and $Al_{85}Fe_{15}$-B Composites with Amorphous or Nanocrystalline-Matrix Produced by Consolidation of Mechanically Alloyed Powders, *Intermetallics*, 2011, **19**, p 1243–1249
5. L. Shaw, H. Luo, J. Villegas, and D. Miracle, Thermal Stability of Nanostructured $Al_{93}Fe_3Cr_2Ti_2$ Alloys Prepared Via Mechanical Alloying, *Acta Mater.*, 2003, **51**, p 2647–2663
6. M. Jafari, M.H. Enayati, M.H. Abbasi, and F. Karimzadeh, Thermal Stability and Structural Changes During Heat Treatment of Nanostructured Al2024 Alloy, *J. Alloy. Compd.*, 2009, **478**, p 260–264
7. S. Mula, S. Ghosh, and S.K. Pabi, Synthesis of an Al-Based Al-Cr-Co-Ce Alloy by Mechanical Alloying and its Thermal Stability, *Mater. Sci. Eng. A*, 2008, **472**, p 208–213
8. S.N. Hosseini, M.H. Enayati, and F. Karimzadeh, Nanoscale Grain Growth Behaviour of CoAl Intermetallic Synthesized by Mechanical Alloying, *Bull. Mater. Sci.*, 2014, **37**, p 383–387
9. J.B. Fogagnolo, D. Amador, E.M. Ruiz-Navas, and J.M. Torralba, Solid Solution in Al-4.5 wt.% Cu Produced by Mechanical Alloying, *Mater. Sci. Eng. A*, 2006, **433**, p 45–49
10. H. Ashrafi, R. Emadi, and M.H. Enayati, Fabrication and Characterization of Nanocrystalline Al/Al12(Fe, V)3Si Alloys by Consolidation of Mechanically Alloyed Powders, *Int. J. Miner. Metall. Mater.*, 2014, **21**, p 711–719
11. H. Ashrafi, M.H. Enayati, and R. Emadi, Mechanical Properties and Thermal Stability of Nanostructured Al/Al12(Fe, V)3Si Alloys Produced by Powder Metallurgy, *J. Mater. Eng. Perform.*, 2014, **23**, p 1780–1789
12. K. Williamson and W.H. Hall, X-ray Line Broadening from Field Aluminum and Wolfram, *Acta Metall.*, 1953, **1**, p 22–31
13. H. Ashrafi, M.H. Enayati, and R. Emadi, Nanocrystalline Al/Al12(Fe, V)3Si Alloy Prepared by Mechanical Alloying: Synthesis and Thermodynamic Analysis, *Adv. Powder Technol.*, 2014, **25**, p 1483–1491
14. B.D. Cullity, *Elements of x-ray Diffraction*, Addison-Wesley, Reading, MA, 1978
15. G.E. Murch, Phase Transformations in Materials, *Materials Science and Technology*, R.W. Cahn, P. Haasen, and E.J. Kramer, Ed., VCH Verlagsgesellschaft mbH, Weinheim, 1991, p 75–141
16. L.S. Shvindlerman and G. Gottstein, Precipitation Accelerated Grain Growth, *Scr. Mater.*, 2004, **50**, p 1051–1054
17. J.R. Groza, Nanocrystalline Powder Consolidation Methods, *Nanostructured Materials*, C. Koch, Ed., William Andrew, Norwich, NY, 2002, p 115–178
18. G.E. Dieter and D.J. Bacon, *Mechanical Metallurgy*, McGraw-Hill Higher Education, New York, 1988
19. L. Shaw, H. Luo, J. Villegas, and D. Miracle, Effects of Internal Strains on Hardness of Nanocrystalline Al-Fe-Cr-Ti Alloys, *Scr. Mater.*, 2004, **51**, p 449–453
20. S.S. Nayak, M. Wollgarten, J. Banhartb, S.K. Pabi, and B.S. Murty, Nanocomposites and an Extremely Hard Nanocrystalline Intermetallic of Al-Fe Alloys Prepared by Mechanical Alloying, *Mater. Sci. Eng. A*, 2010, **527**, p 2370–2378
21. Y. Du, Y.A. Chang, B. Huang, W. Gong, Z. Jin, H. Xu, Z. Yuan, Y. Liu, Y. He, and F.Y. Xie, Diffusion Coefficients of Some Solutes in fcc and Liquid Al: Critical Evaluation and Correlation, *Mater. Sci. Eng. A*, 2003, **363**, p 140–151